International Journal of Nanomedicine

Dovepress
open access to scientific and medical research

Open Access Full Text Article

ORIGINAL RESEARCH

Controlled Quercetin Release by Fluorescent Mesoporous Nanocarriers for Effective Anti-Adipogenesis

Taelin Kim*, A Yeon Cho*, Sang-Wha Lee, Hyun Jong Lee

School of Chemical, Biological and Battery Engineering, Gachon University, Seongnam-si, Gyeonggi-do, Republic of Korea

*These authors contributed equally to this work

Correspondence: Sang-Wha Lee; Hyun Jong Lee, School of Chemical, Biological and Battery Engineering, Gachon University, Seongnam-si, Gyeonggi-do, Republic of Korea, Email lswha@gachon.ac.kr; hjlee2@gachon.ac.kr

Introduction: Quercetin (QUER), a flavonoid abundant in fruits and vegetables, is emerging as a promising alternative therapeutic agent for obesity treatment due to its antioxidant and anti-adipogenic properties. However, the clinical application of QUER is limited by its poor solubility, low bioavailability, and potential toxicity at high doses. To address these challenges, this study aims to develop an advanced drug delivery system using fluorescent mesoporous silica nanoparticles (FMSNs) coated with polydopamine (PDA) for the efficient and sustained delivery of QUER to inhibit adipogenesis.

Methods: The research included the synthesis of PDA-coated FMSNs for encapsulation of QUER, characterization of their mesoporous structures, and systematic investigation of the release behavior of QUER. The DPPH assay was used to evaluate the sustained radical scavenging potential. Concentration-dependent effects on 3T3-L1 cell proliferation, cellular uptake and adipogenesis inhibition were investigated.

Results: PDA-coated FMSNs exhibited well-aligned mesoporous structures. The DPPH assay confirmed the sustained radical scavenging potential, with FMSNs-QUER@PDA showing 53.92 ± 3.48% inhibition at 72 h, which was higher than FMSNs-QUER (44.66 ± 0.57%) and free QUER (43.37 ± 5.04%). Concentration-dependent effects on 3T3-L1 cells highlighted the enhanced efficacy of PDA-coated FMSNs for cellular uptake, with a 1.5-fold increase compared to uncoated FMSNs. Adipogenesis inhibition was also improved, with relative lipid accumulation of 44.6 ± 4.6%, 37.3 ± 4.6%, and 36.5 ± 7.3% at 2.5, 5, and 10 μM QUER concentrations, respectively.

Conclusion: The study successfully developed a tailored drug delivery system, emphasizing sustained QUER release and enhanced therapeutic effects. FMSNs, especially when coated with PDA, exhibit promising properties for efficient QUER delivery, providing a comprehensive approach that integrates advanced drug delivery technology and therapeutic efficacy.

Keywords: mesoporous silica nanoparticles, quercetin, polydopamine coating, drug delivery system, adipogenesis inhibition, sustained release

Introduction

The escalating global prevalence of obesity, with more than 1.9 billion adults and 650 million people classified as obese, has created a critical health crisis.[1] This pervasive problem spans all age groups and is strongly associated with an increased risk of chronic disease, placing a significant burden on healthcare systems.[2] Adipogenesis, the process that leads to fat accumulation, is a central target in fight against obesity. Current interventions often rely on synthetic drugs, raising concerns about long-term safety and sustainability.[3,4] Against this backdrop, the exploration of natural compounds with anti-adipogenic properties is gaining prominence, in line with the global trend towards sustainable health solutions.[5]

Existing strategies to inhibit adipogenesis are predominantly based on synthetic drugs, a paradigm with limitations.[3,6] While these pharmaceutical interventions have some degree of efficacy, they often have significant drawbacks. The

Received: 11 February 2024
Accepted: 22 May 2024
Published: 8 June 2024

Graphical Abstract

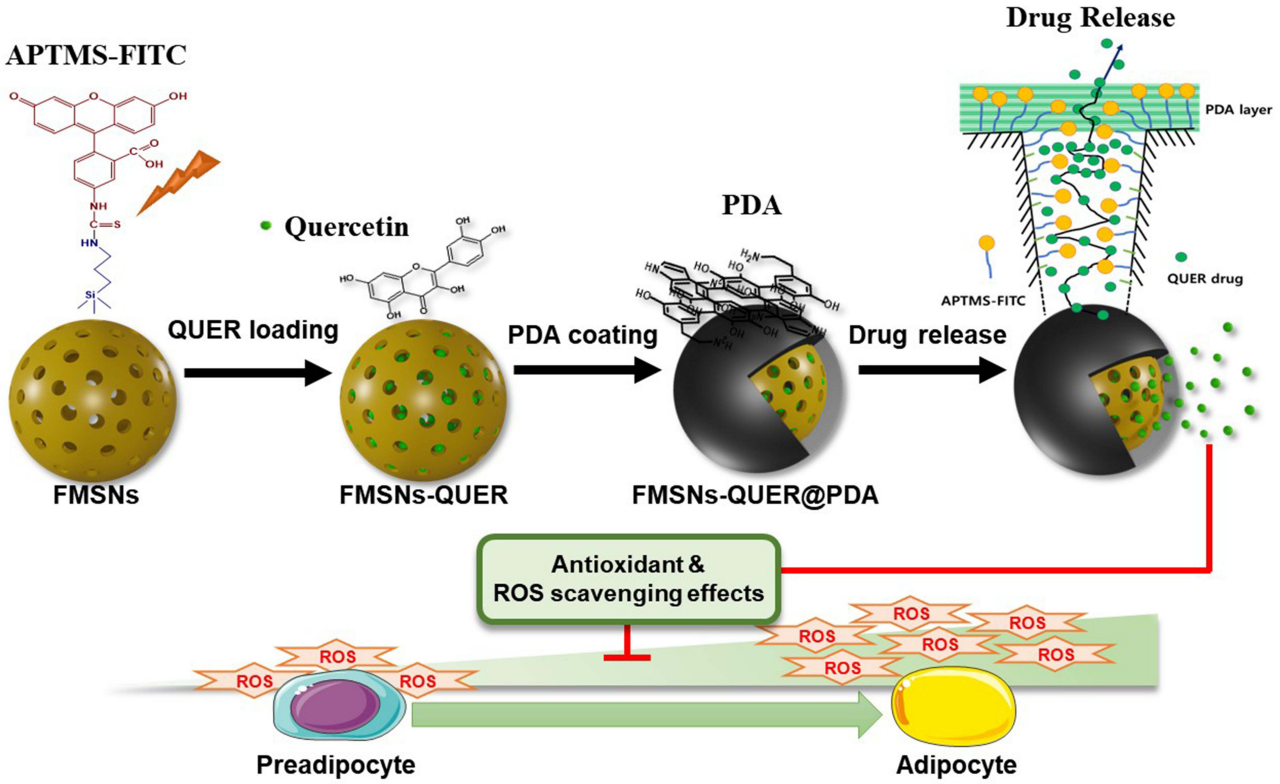

synthetic nature of these drugs raises concerns about potential side effects and long-term safety, limiting their viability for chronic diseases such as obesity.[3,7] In addition, the cost implications associated with pharmaceutical solutions contribute to their limited accessibility, hindering widespread adoption. As the need for sustainable healthcare solutions increases, a shift to natural compounds becomes imperative.

Quercetin (QUER), a flavonoid abundant in fruits and vegetables, is emerging as a promising alternative.[8,9] Its natural origin not only circumvents synthetic concerns, but also addresses the growing demand for affordable and side-effect-free interventions in the area of adipogenesis inhibition.[10] Its unique chemical structure, characterized by a dihydroxylation pattern on the benzene ring, contributes to its enhanced bioactivity and multiple physiological benefits.[11] QUER exhibits superior antioxidant properties, effectively scavenging free radicals and mitigating oxidative stress.[12] In addition, its exceptional bioavailability and metabolic stability enhance its therapeutic potential. This compound's ability to modulate cellular signaling pathways associated with adipogenesis inhibition distinguishes it as a potent natural agent for addressing obesity-related problems.[13] Leveraging these distinctive attributes, our study focuses on exploring the efficacy of QUER in the sustained inhibition of adipogenesis, providing a valuable alternative to other flavonoids with more limited bioactive profiles.

However, the clinical use of QUER is often hampered by its poor solubility in the aqueous phase, low hydrolytic stability at neutral (or alkaline) pH, and limited bioavailability.[14,15] Encapsulation technology improves the stability and bioavailability of QUER.[16,17] Although QUER is generally considered safe, it can be toxic at high concentrations.[18,19] Therefore, in order to achieve the desired effects, such as antioxidant activity, while ensuring cellular protection, a delivery system capable of sustained release is required, rather than delivering a large amount at once.

In recent years, various nanoparticulate delivery systems have been explored to improve the efficacy and specificity of anti-adipogenic compounds. Polymeric nanoparticles, such as those based on poly(lactic-co-glycolic acid) (PLGA), have

been used to deliver QUER.[20] Similarly, lipid-based nanoparticles, including solid lipid nanoparticles (SLNs) and nanostructured lipid carriers (NLCs), have shown promise in delivering QUER.[21–24]

Mesoporous silica nanoparticles (MSNs) have emerged as promising carriers for the enhanced delivery of poorly water-soluble compounds such as QUER. MSNs possess high surface area, tunable pore size, and biocompatibility, making them versatile platforms for encapsulation and delivery of various bioactive agents.[25,26] Their porous structure allows for controlled release of the cargo, contributing to prolonged therapeutic effects and minimizing side effects. To further enhance the efficacy of MSNs, a polydopamine (PDA) layer can be applied to their surfaces, potentially improving their biocompatibility and cellular uptake.[27–29]

This study aims to develop and evaluate a versatile drug delivery system using mesoporous nanocarriers to improve the delivery and therapeutic efficacy of QUER while inhibiting adipogenesis. The incorporation of QUER into PDA-coated fluorescent MSNs (FMSNs) provides a dual advantage by improving the stability of QUER and enabling sustained release by exploiting the inherent antioxidant properties of PDA. This synergistic approach not only addresses the limitations of QUER, but also enhances its therapeutic potential. A comprehensive investigation includes physicochemical characterization, drug release kinetics, antioxidant activity, cellular uptake, and inhibition of adipocyte differentiation. These analyses deepen our understanding of the interactions between QUER, FMSNs, and PDA and shed light on their roles in enhancing drug delivery and modulating adipogenesis. This study provides detailed insights into the design principles, fabrication methods, and behavior of QUER-loaded and PDA-coated FMSNs.

Materials and Methods

The following chemicals and materials were used in this study: tetraethyl orthosilicate (TEOS, 99%, CAS: 78–10-4), cetyltrimethylammonium bromide (CTAB, 99%, CAS: 57–09-0), ammonium fluoride (NH_4F, 99.99%, CAS: 12,125–01-8), 3-aminopropyl-trimethoxysilane (APTMS, 97%, CAS: 13,822–56-5), fluorescein isothiocyanate (FITC, 90%, CAS: 3326–32-7), dopamine hydrochloride (DA, 99%, CAS: 62–31-7), quercetin (QUER, 98%, CAS: 117–39-5), insulin (CAS: 11,061–68-0), 3-isobutyl-1-methylxanthine (IBMX, CAS: 28,822–58-4), dexamethasone (CAS: 50–02-2), paraformaldehyde (CAS: 30,525–89-4), isopropanol (CAS: 67–63-0), and dimethylsulfoxide (DMSO, CAS: 67–68-5) from Sigma–Aldrich Co. (St. Louis, MO, USA). Ethanol (99.5%, Cat. No. 0777–00081) and hydrochloric acid (HCl, 36%, Cat. No. H1469) were obtained from Daejung Co. (Siheung, Korea) and Samchun (Seoul, Korea), respectively. Deionized (DI) water (HPLC grade, CAS: 7732–18-5) and phosphate-buffered saline (PBS, Cat. No. 2,540,093) were purchased from J. T. Baker. Co. (Phillipsburg, NJ, USA) and Bioneer (Daejeon, Korea), respectively.

Cell culture reagents, including Dulbecco's modified Eagle medium (DMEM), bovine calf serum (BCS), fetal bovine serum (FBS), penicillin, and 3-(4,5-dimethylthiazol-2-yl)-2,5-diphenyltetrazolium bromide (MTT) were purchased from Thermo Fisher Scientific (Waltham, MA, USA). The Oil Red O staining kit (Cat. No. 0843-SC) and the DPPH (2,2-diphenyl-1-picrylhydrazyl) antioxidant assay kit (Cat. No. D678) were obtained from Science Cell (Carlsbad, CA, USA) and Gerbu (Heidelberg, Germany), respectively. All chemicals and reagents were used as received without further purification.

Synthesis of Mesoporous Silica Nanoparticles

MSNs were synthesized using a modified Stober method. Briefly, CTAB (0.15 g) and NH_4F (0.4 g) were dissolved in 100 mL of deionized (DI) water and stirred at 1500 rpm for 1 h at 80 °C. TEOS (2 mL) was then added dropwise to the solution, resulting in a milky mixture. The reaction was allowed to proceed for 2 h at 80 °C. The resulting product was collected by centrifugation at 8500 rpm for 8 min and washed several times with DI water and ethanol. To remove the CTAB template, the product was dispersed in ethanol containing HCl (37%) at a volume ratio of 60:1 (ethanol:HCl) and stirred at 80 °C for 4 h. This process was repeated twice. The final product was recovered by centrifugation, washed with ethanol, and dried at 60 °C for 24 h in the dark.

FMSNs were prepared by incorporating an APTMS-FITC (A-F) complexes during the synthesis process. The A-F complex was prepared by dissolving FITC (2.5 mg) and APTMS (0.12 mL) in 3 mL of ethanol and stirring continuously for 6 h at room temperature. The A-F complex solution was then kept at 4°C for 18 h prior to use. FMSNs were synthesized following the same procedure as for MSNs, with the addition of the A-F complex to the milky mixture

after TEOS addition. The reaction was carried out at 80 °C for 24 h in the dark. The resulting yellow product was collected by centrifugation, washed several times with water and ethanol, and subjected to the same CTAB removal process as described for MSNs. The final FMSNs were obtained after drying at 60 °C for 24 h in the dark.

Preparation of Polydopamine-Coated Nanocarriers

PDA coating was applied to the QUER-loaded FMSNs (FMSNs-QUER) through the oxidative polymerization of dopamine under alkaline conditions, as described previously with slight modifications.[30] Briefly, 100 mg of FMSNs-QUER were dispersed in 10 mL of Tris-(hydroxymethyl)aminomethane-HCl buffer (Tris-HCl, pH 8.5). Dopamine hydrochloride (10 mg) was added to the FMSNs-QUER dispersion and allowed to react at room temperature for 3 h under stirring in the dark. The PDA-coated FMSNs-QUER (FMSNs-QUER@PDA) were collected by centrifugation at 8500 rpm for 10 min and washed three times with deionized water to remove any residual impurities. The samples were then freeze-dried for 24 h and stored in the dark until further use. The synthesized samples were characterized using scanning electron microscopy (SEM, SU8600, Hitachi, Japan) and transmission electron microscopy (TEM, Tecnai, FEI, Hillsboro, OR, USA) at the Smart Materials Research Center for IoT at Gachon University.

Drug Loading and Characterization of Quercetin-Loaded Nanocarriers

To load QUER into the MSNs and FMSNs, the nanoparticles were dispersed in dimethyl sulfoxide (DMSO) containing QUER and stirred continuously for 24 h in the dark. The drug-loaded nanocarriers were collected by centrifugation at 8500 rpm for 10 min. Excess drug adsorbed onto the particle surface was removed by washing with deionized water. The QUER-loaded nanocarriers were then freeze-dried for 24 h. Due to its hydrophobic nature, QUER has a weak tendency to escape from the particles.

The drug loading capacity of each nanocarrier was determined by measuring the change in absorbance of QUER in the loading solution before and after the loading process. The amount of loaded and lost QUER was calculated using standard calibration curves (Figure S1). The calibration curves were obtained by measuring the absorbance of QUER in DMSO (concentration range: 5–30 μg/mL) at 374 nm (Figure S1a) and in Tris-HCl buffer (pH 8.5, concentration range: 5–30 μg/mL) at 284 nm (Figure S1b).[31,32] All calibration curves exhibited good linearity with R^2 values greater than 0.999.

The loading amounts of QUER in MSNs and FMSNs were found to be 43 and 105 mg/g (mg drug/g particle), respectively (Table 1). The lower loading capacity of MSNs can be attributed to the electrostatic repulsion between the negatively charged MSNs and anionic QUER molecules. In contrast, the A-F complex grafted onto the FMSNs possesses a positive charge, resulting in a higher loading capacity due to the electrostatic attraction between the nanoparticles and QUER. After PDA coating, the loading capacity of FMSNs@PDA decreased to 91.6 mg/g, exhibiting a reduction of 12.8 wt%. This decrease is likely caused by the loss of encapsulated drug during the PDA coating process. The volume of all solutions used in the loading and washing processes was maintained at 10 mL.

In vitro Quercetin Release Study

The release profile of quercetin (QUER) from the nanocarriers was investigated under different pH conditions, simulating the physiological environment. The study was conducted at pH 7.4 (representing the neutral pH of blood and normal cells) and pH 5.5 and 4.0 (mimicking the acidic conditions found in endosomes and lysosomes, respectively).[33,34]

Briefly, 30 mg of QUER-loaded nanoparticles (MSNs-QUER, FMSNs-QUER, or FMSNs-QUER@PDA) were suspended in 10 mL of phosphate-buffered saline (PBS) at the desired pH. The suspensions were maintained at 37 ± 1 °C under gentle stirring. At predetermined time intervals (every hour), an aliquot of the release medium (1 mL) was withdrawn and replaced with an equal volume of fresh PBS to maintain sink conditions. The aliquots were centrifuged at 12,000 rpm for 5 min to remove any suspended nanoparticles. The concentration of released QUER in the supernatant was determined by measuring the absorbance at 374 nm using a UV-Vis spectrophotometer. The cumulative release percentage of QUER was calculated based on the total amount of drug loaded in the nanoparticles.

The release experiments were performed in triplicate for each pH condition and nanocarrier type. The release profiles of QUER from MSNs, FMSNs, and FMSNs@PDA were compared to evaluate the effect of nanocarrier composition and surface modification on the drug release kinetics.

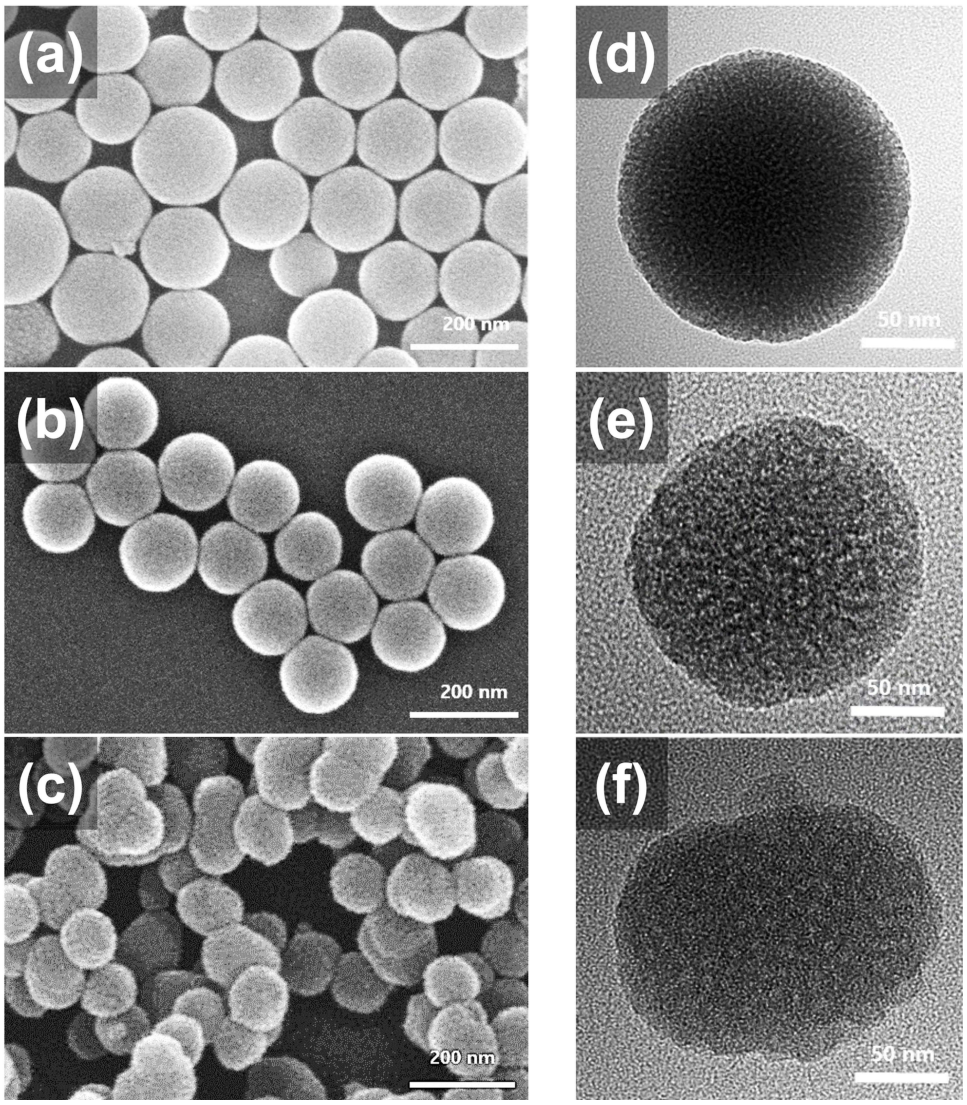

Figure 1 Morphological characterization of the synthesized nanoparticles. SEM images of (**a**) MSNs, (**b**) FMSNs, and (c) FMSNs@PDA. TEM images of (**d**) MSNs, (**e**) FMSNs, and (**f**) FMSNs@PDA.

Evaluation of the Antioxidant Activities of Quercetin

The antioxidant capacity of QUER and QUER-loaded nanocarriers was assessed using DPPH assay. DPPH is a stable free radical widely employed in antioxidant assays due to its ability to accept electrons or hydrogen radicals, providing a reliable measure of the free radical scavenging activity of compounds.

Table 1 Amounts of Quercetin (QUER) Loaded in MSNs, FMSNs and FMSNs@PDA After Surface Modification

As-prepared sample	MSNs-QUER	FMSNs-QUER	FMSNs-QUER@PDA
Initial amounts of drug in the solution before drug loading process (mg/mL)[a)]	30	30	30
Residual amounts of the drug in the solution after drug loading (mg/mL)[b)]	29.44	28.92	28.92
Drug loss amount in the washing solution after surface modification (mg/mL)[c)]	0.124	0.023	0.164
Final loading amount of the drug in the particle (mg/g)[d)]	43.6	105	91.6 (Loss 12.8%)

Notes: [a)]Amount of drug dissolved in DMSO before drug loading [b)] Amount of drug dissolved in DMSO after drug loading [c)] Amount of drug lost during washing and coating process [d)] Amount of drug loaded per g of nanoparticle.

The DPPH antioxidant assay was performed following the manufacturer's instructions for the assay kit. Briefly, a DPPH working solution (100 μL, 0.2 mM in ethanol) was mixed with 100 μL of the sample solution (free QUER, FMSNs-QUER, FMSNs-QUER@PDA, FMSNs, or FMSNs @PDA) at various time points (0, 6, 24, 48, and 72 h). This approach allows for the evaluation of the antioxidant efficacy of the compounds over different time periods. The mixtures were incubated for 30 minutes at 25 °C in the dark. Subsequently, the absorbance of each sample was measured at 517 nm using a microplate reader.

The DPPH radical scavenging activity was calculated using the following equation:

DPPH radical scavenging activity (%) = [(Abs_control - Abs_sample) / Abs_control] × 100

where Abs_control is the absorbance of the DPPH solution without the sample, and Abs_sample is the absorbance of the DPPH solution with the sample.

The antioxidant activity of free QUER and QUER-loaded nanocarriers was compared to evaluate the effect of nanoencapsulation and surface modification on the antioxidant capacity of QUER over time.

Evaluation of the Effect of Nanocarriers on Cell Behavior

3T3-L1 fibroblasts (Korea Cell Line Bank, Seoul, South Korea) were cultured in DMEM supplemented with 10% BCS and 1% penicillin at 37 °C in a humidified atmosphere containing 5% CO_2.

The effect of QUER and QUER-loaded nanoparticles on 3T3-L1 cell proliferation was assessed using MTT assay. Briefly, 8×10^3 cells were seeded into each well of a 24-well plate and grown until confluence was reached. The cells were then treated with various concentrations (2.5, 5, or 10 μM) of QUER, FMSNs-QUER, or FMSNs-QUER@PDA, and the media was changed every two days. On days 1, 4, and 7, MTT solution (5 mg/mL in PBS) was added to each well at a ratio of 1:10 to the medium, and the cells were incubated for 4 h at 37 °C. The formazan crystals were dissolved in 650 μL of dimethyl sulfoxide (DMSO), and the absorbance was measured at 540 nm using a microplate reader (BioTek, Winooski, VT, USA).

To evaluate the cellular uptake of nanoparticles, 8×10^3 3T3-L1 cells were seeded into each well of a 24-well plate and treated with FMSNs or FMSNs@PDA at a concentration corresponding to 10 μM of QUER. The media was changed every two days. On days 1, 2, 4, and 6, the cells were observed under a fluorescence microscope (Olympus IX71, Tokyo, Japan), and the cellular uptake area was quantified using ImageJ software (NIH, Bethesda, MD, USA).

Post-confluent 3T3-L1 cells were differentiated into adipocytes by treatment with DMEM containing 10% FBS, 10 μg/mL insulin, 0.5 mM IBMX, and 1 μM dexamethasone. For the first four days, cells were maintained in DMEM supplemented with 10% FBS and 10 μg/mL insulin, with a media change on day 2. From day 4 onwards, cells were cultured in DMEM containing 10% FBS for an additional two days to complete differentiation.

On day 8 of differentiation, the cells were washed twice with PBS and fixed with 4% paraformaldehyde solution for 30 min at room temperature. After washing with 60% isopropanol, the cells were stained with Oil Red O working solution (prepared by diluting Oil Red O stock solution with distilled water at a ratio of 6:4) for 15 min. The stained cells were washed three times with distilled water and observed under a microscope. For quantification of lipid accumulation, the cells were washed three times with 60% isopropanol, and the incorporated Oil Red O was eluted with 100% isopropanol. The absorbance was measured at 490 nm using a microplate reader.

Statistical Analysis

All experiments were conducted in triplicate unless otherwise specified, and the results were expressed as mean ± standard deviation. Statistical analysis was performed using GraphPad Prism 10 software (San Diego, CA, USA). Comparisons among multiple groups were carried out by one-way analysis of variance (ANOVA) followed by Tukey's post hoc test for pairwise comparisons. A p-value of less than 0.05 was considered statistically significant.

Results and Discussion

A nanoparticle designed for the sustained release of QUER was synthesized to inhibit adipogenesis. These particles were designed to encapsulate QUER within FMSNs and were further modified with PDA coating to regulate the release

kinetics of QUER. This tailored system allows for a controlled and gradual release of QUER, enhancing its efficacy in inhibiting adipogenesis.

The synthesized samples were characterized using SEM and TEM. Figure 1a shows an SEM image of spherical MSNs with a uniform size of ~150 nm. The corresponding TEM image reveals the well-ordered mesoporous structure of the MSNs (Figure 1d). The FMSNs exhibit a similar spherical morphology and uniform size distribution to the MSNs (Figure 1b). The mesoporous structure with distinct pores is clearly visible in the TEM image of the FMSNs (Figure 1e). Figure 1c shows an SEM image of FMSNs@PDA, which displays a rough surface morphology, likely due to the presence of the PDA coating layer. The TEM image of FMSNs@PDA further confirms the rough surface and the retention of the mesoporous structure (Figure 1f).

To confirm the surface modification and colloidal stability of the mesoporous nanocarriers, the hydrodynamic sizes and zeta potentials of the samples were measured using an electrophoretic light scattering (ELS), and the results are summarized in Table S1. The average hydrodynamic diameters of the MSNs, FMSNs, and FMSNs@PDA in PBS (0.5 mg/mL, pH 7.4) were found to be 150 ± 30 nm, 155 ± 22 nm, and 164 ± 39 nm, respectively. The gradual increase in the size of the nanoparticles can be attributed to the surface modifications, such as the grafting fluorescent A-F complex (from 150 to 155 nm) and the subsequent PDA coating (from 155 to 164 nm). These changes in the nanoparticle size confirm the successful surface modification step. The zeta potentials of the MSNs and FMSNs were measured to be −31.53 ± 1.96 mV and −21.12 ± 2.31 mV at pH 7.4, respectively. The slight increase in the zeta potential of the FMSNs towards a more positive value can be ascribed to the grafting of the positively charged A-F complex.[35] In contrast, the zeta potential of FMSNs@PDA decreased to −45.16 ± 1.45 mV at pH 7.4 in PBS buffer, which can be attributed to the presence of phenolic groups in the PDA layer. These groups exist in their quinone form at neutral pH, resulting in a more negative zeta potential.[36]

To provide a comprehensive characterization, we performed zeta potential measurements on FMSNs@PDA samples in HPLC water at different pH values adjusted by HCl and NaOH agents. As depicted in Figure S2, these particles exhibited a positive zeta potential of 19.29 ± 2.48 mV at acidic pH 3. As the pH of the solution increased, there was a notable decline in the zeta potential, reaching a negative value of −19.37 ± 2.84 mV at pH 5.0. Subsequently, the zeta potential further decreased under neutral and basic pH conditions and finally reached to a highly negative value of −63.31 ± 3.34 mV at pH 11. The amphiphilic nature of PDA, characterized by its phenolic and amine functional groups, governs its zeta potential behaviour.[36] In acidic conditions, protonation of amine groups leads to a positive zeta potential, whereas in neutral and basic conditions, deprotonation of phenolic groups results in a negative zeta potential. Our investigation demonstrates the typical pattern of zeta potential shifts in PDA-coated particles, displaying a reversal from positive to negative values and a consistent decrease across the pH from 3 to 11.[37] These observations clearly confirm the presence of PDA on the particle surface.

The as-synthesized samples (MSNs, FMSNs, and FMSNs@PDA) were characterized using Fourier-transform infrared (FT-IR) spectroscopy, X-ray diffraction (XRD), and photoluminescence (PL) spectroscopy to confirm the successful surface modifications and investigate their structural properties.

The FT-IR spectra of the MSNs (Figure 2a), exhibit characteristic peaks at 1092 cm^{-1} and 800 cm^{-1}, corresponding to the stretching and asymmetric vibrations of Si-O-Si bonds, respectively. The asymmetric vibration of Si-OH is observe at 970 cm^{-1}, which can be attributed to the -OH stretching vibration of the silanol group and its adsorbed water. The FMSNs show additional peaks at 1480 cm^{-1} and 1640 cm^{-1}, assigned to the C-O and C=C bond oscillations of the grafted A-F complex, respectively. The presence of peaks at 2900 cm^{-1} and 2850 cm^{-1}, corresponding to the asymmetric and symmetric stretching vibrations of the CH_2 group, further confirms the successful conjugation of the A-F complex. The FMSNs@PDA exhibit a broad OH/NH band ranging from 3600 to 3000 cm^{-1}, which is more pronounced than that observed in the FMSNs. Additionally, a new peak at 1650 cm^{-1}, attributed to the -NH groups in the aromatic ring, verifies the successful coating of the PDA layer.

The XRD patterns of the MSNs and FMSNs display well-resolved peaks in the (1 0 0) direction, but not in the (1 1 0) and (2 0 0) directions, suggesting a hexagonal symmetry and a well-ordered arrangement of pores in the mesoporous nanoparticles (Figure 2b).[38,39] The FMSNs exhibit a decrease in diffraction peaks, with a slight shift from (1 0 0) towards higher 2θ values. This indicates that the pore structure remains intact even with the inclusion of the A-F complex during

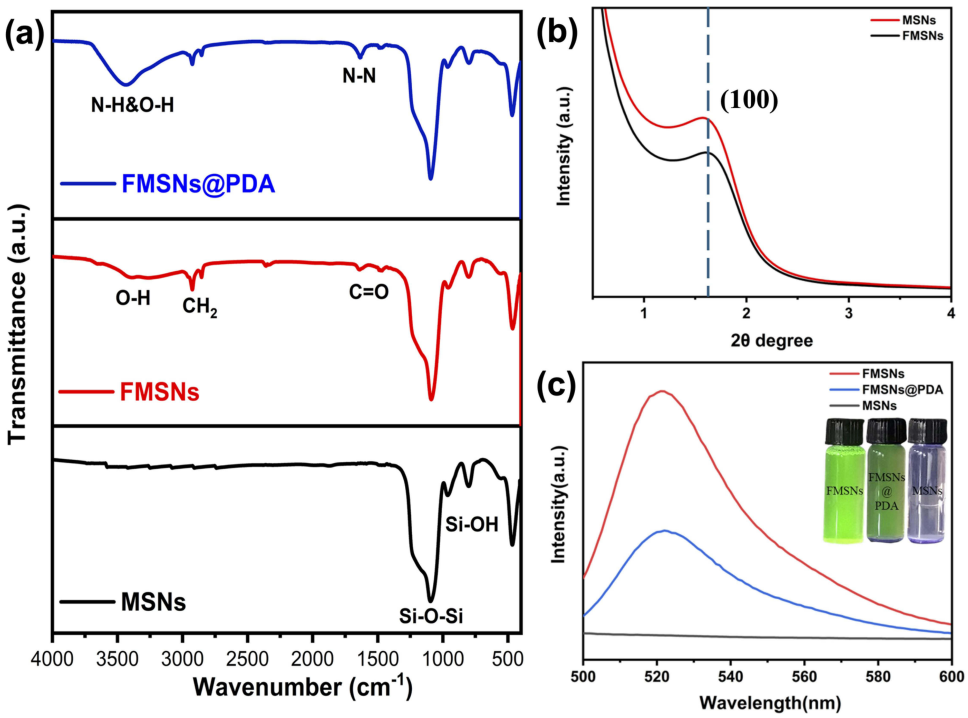

Figure 2 (**a**) FT-IR spectra, (**b**) XRD spectra, and (**c**) photoluminescence spectra of the as-prepared samples (MSNs, FMSNs, and FMSNs@PDA).

the particle synthesis process. Furthermore, the decrease in peak intensity is attributed to the scattering force exerted by the silica walls grafted with functional organic molecules with disordered/ordered species.[40]

The PL spectra reveal that while the MSNs do not exhibit any fluorescence, the FMSNs and FMSNs@PDA show distinct emission peaks at 522 nm (Figure 2c). The FMSNs display a higher fluorescence intensity compared to the FMSNs@PDA, which can be attributed to the presence of the PDA layer that partially absorbs and blocks the fluorescent light emitted by the FMSNs upon excitation. The inset in Figure 2c shows the intense green and dark green fluorescence of the FMSNs and FMSNs@PDA, respectively, confirming the successful grafting of the FITC-containing A-F complex and PDA coating layer onto the FMSNs. The FITC-conjugated nanocarriers enable real-time fluorescent monitoring of the delivery routes and can confirm the successful transport of the drug to the target area.

The nitrogen adsorption/desorption isotherms and pore size distributions of the samples, obtained using the Brunauer–Emmett–Teller (BET) and Barrett–Joyner–Halenda (BJH) methods, are presented in Figure S3 and Table S2, respectively. The samples exhibit type IV isotherms, characteristic of porous materials with a constant cross-section.[41] The BET surface area and pore size of the MSNs (Figure S3a) are calculated to be 84.51 m^2/g and 9.76 nm, respectively. The FMSNs (Figure S3b) show an increased surface area (127.36 m^2/g) and pore sizes (17.11 nm), likely due to the grafting of the brush-like A-F complex on the pore walls. After coating the FMSNs with PDA (Figure S3c), the surface area of the resulting FMSNs@PDA further increased to 156.55 m^2/g, while the pore size slightly decreased to 16.70 nm, probably due to the pore-blocking effect by the PDA layer.[42] The shape of the adsorption/desorption isotherm and the type of hysteresis loop remain unchanged for all samples, indicating the retention of the mesoporous structure despite the surface modification steps (A-F complex grafting and PDA coating).

Investigation of drug release kinetics is crucial for understanding the behavior of drug delivery systems and optimizing their performance. In this study, we evaluated the drug release profiles of mesoporous nanocarriers loaded with QUER. Figure 3 illustrates the time-course release of QUER from the nanocarriers (MSNs, FMSNs and FMSNs@PDA) in PBS under different pH conditions (pH 7.4, 5.5, and 4.0).

Figure 3a shows the release profiles of QUER from MSNs, demonstrating a consistent release rate regardless of pH levels, with an observed release fraction of ~80% within 10 h. Figure 3b represents the release profiles of FMSNs-QUER, showing the more retarded release of QUER compared to MSNs-QUER. At pH 4.0, FMSNs-QUER exhibited a release

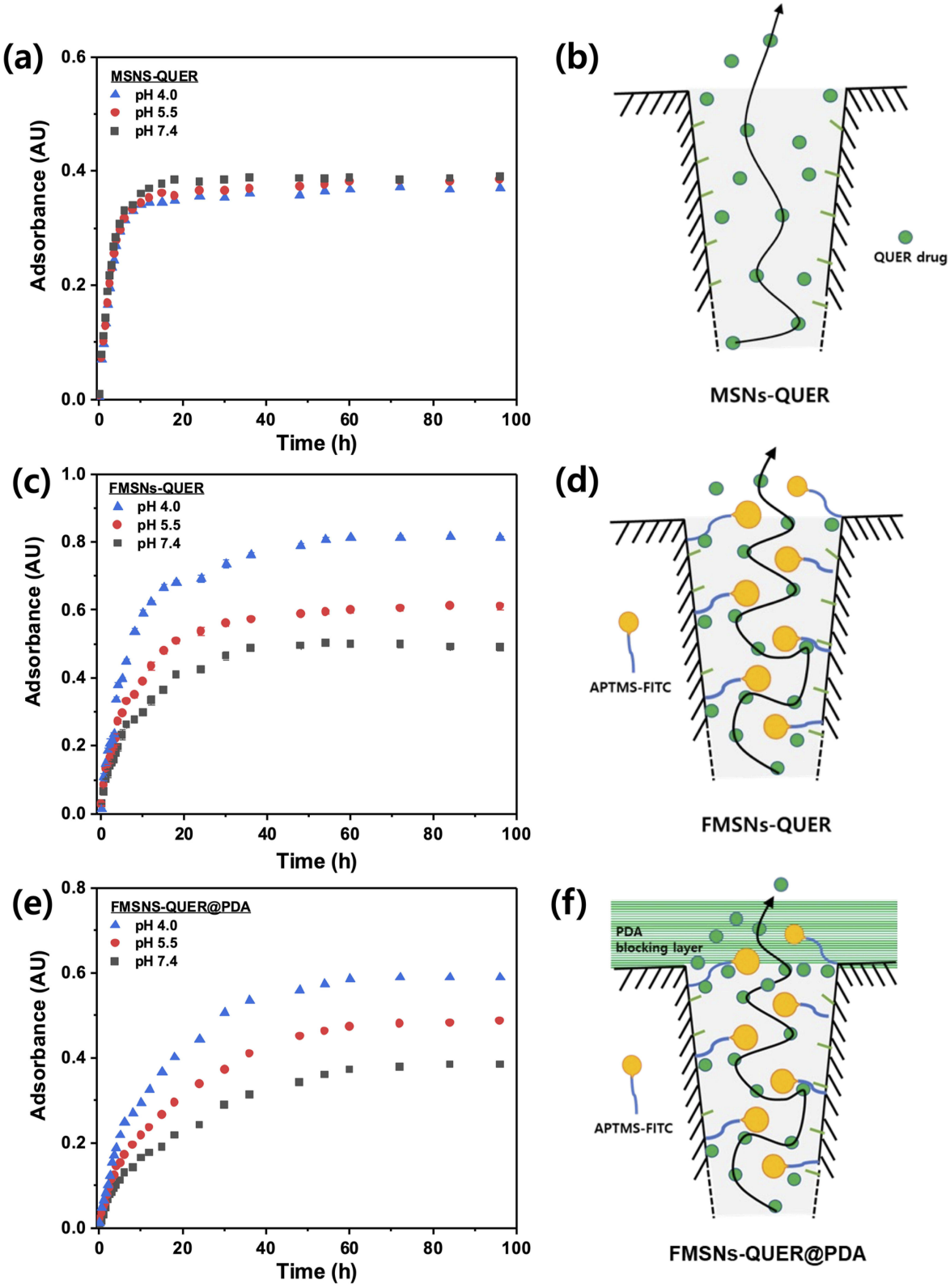

Figure 3 Release profiles of QUER from (**a**) MSNs-QUER, (**b**) FMSNs-QUER and (**c**) FMSNs-QUER@PDA. Schematic illustrations of the release mechanism for (**d**) MSNs-QUER, (**e**) FMSNs-QUER, and (**f**) FMSNs-QUER@PDA, depicting the influence of the A-F complex and PDA layer on drug release.

fraction of 83.85% within 15 h, gradually approaching a saturation value thereafter. At pH 5.5, a release fraction of 77.13% was obtained within 5 h, while at pH 7.4, a release fraction of 65.21% was observed within the same time. These results indicate that drug release is more pronounced under acidic conditions (pH 4.0). The acidic pH plays a crucial role in preserving the structural integrity of QUER, preventing significant degradation or modification. In contrast, under neutral or strong basic conditions, the γ-pyrone fragment of QUER is prone to hydrolytic degradation, particularly in alkaline pH conditions, leading to fragmentation or alteration of the QUER structure.[31,32] Figure 3c displays the release profiles of FMSNs-QUER@PDA, showing release fractions of 74.02%, 91.95%, and 99.43% at pH 7.4, pH 5.5, pH 4.0, respectively. FMSNs-QUER@PDA showed a release fraction of ~75% within 24 h, indicating the most delayed release compared to MSNs-QUER (91%), and FMSNs-QUER (85%), owing to the presence of the PDA coating layer.

Figure 3d-f outlines the schematic drug release mechanisms from each nanocarriers. In MSNs-QUER, the electrostatic repulsion between the negatively charged silica and the drug facilitates rapid drug release through the porous channels, without exhibiting pH-responsive controlled release (Figure 3d).[43] Conversely, FMSNs-QUER inhibit drug escape through the brush-like hurdles imposed by the A-F complex grafted on the pore walls (Figure 3e).[40] Additionally, electrostatic attraction occurs between the A-F complex and the drug, providing a further delay effect.[44] QUER undergoes electrostatic and hydrogen-bonding interactions with the positively charged A-F complexes within the porous channels.[45] The increased electrostatic attraction between the anionic QUER and the positively charged A-F complexes decelerates the release rate of the drug. In FMSNs-QUER@PDA, QUER undergoes π-π stacking/hydrogen bonding interactions with the PDA coating layer, which serves as a blocking layer, demonstrating the most pronounced delay in drug transmission (Figure 3f).[46–48] As the pH of the release medium changes from pH 7.4 to pH 4.0, however, the QUER molecule becomes less negative due to the consecutive protonation of multiple -OH groups. As a result, there is an increase of release rate due to the reduced electrostatic attraction between the drug and the A-F complex.[49] In addition, amine groups in the PDA layer become protonated in acidic conditions, and the oxidation of PDA reduces density and delocalization of π electrons, thereby weakening the π-π stacking interaction. This contributes to a further increased release rate of the drug under acidic pH conditions.[50–52]

Evaluating the DPPH radical-scavenging activity allows for the assessment of a sample's ability to neutralize chemically induced radicals, elucidating its free radical-scavenging capability and hydrogen-donating potential. This method is based on the reduction of DPPH, which is characterized by its deep purple color, to DPPH-H. This structural change manifests as a discernible color shift, indicating the antioxidant activity of the test substance.[53] In this study, each sample solution at a concentration of 10 μM was reacted with DPPH at various intervals (0, 6, 24, 48, and 72 h), and the absorbance at 517 nm, reflecting the antioxidant effect, was then measured. Increased antioxidant potency is correlated with increased DPPH radical scavenging, resulting in a lighter coloration and decreased absorbance.

As shown in Figure 4, QUER exhibited the most robust antioxidant efficacy at the 0 and 6 h, whereas the groups with or without released QUER exhibited significantly lower antioxidant efficacy. Notably, the antioxidant effect of QUER decreased over time, with a significant reduction occurring at 24 h, reaching a value of 43.37 ± 5.04% at 72 h. The antioxidant potential of FMSNs without QUER and the inherent antioxidant activity of FMSNs@PDA particles were also characterized. The bare particles exhibit poor antioxidant properties. After PDA coating, a slightly increased inhibition rate was observed compared to bare FMSNs, reaching 19.35 ± 1.92% and 28.28 ± 1.88% at 72 h, respectively. In addition, the antioxidant efficacies of FMSNs-QUER and FMSNs-QUER@PDA showed consistent increasing trends over the observation period. At 72 h, their radical-scavenging potentials reached 44.66 ± 0.57% and 53.92 ± 3.48%, respectively. Notably, FMSNs-QUER@PDA exhibited higher radical-scavenging activity and superior persistence in antioxidant performance compared to FMSN-QUER and free QUER.

In a physiological context, certain radicals play a vital role in facilitating the delivery of oxygen. However, the excessive generation of free radicals leads to the oxidation of various molecules, thereby inducing oxidative damage to macromolecules, such as DNA and proteins.[54] This phenomenon, known as oxidative stress, causes degenerative conditions, including inflammatory diseases and aging. Therefore, the ability of antioxidants to scavenge free radicals is crucial. This radical-scavenging ability has a profound relationship with adipogenesis inhibition, providing a link between the cellular redox balance and the intricate regulation of adipogenesis inhibition.[55]

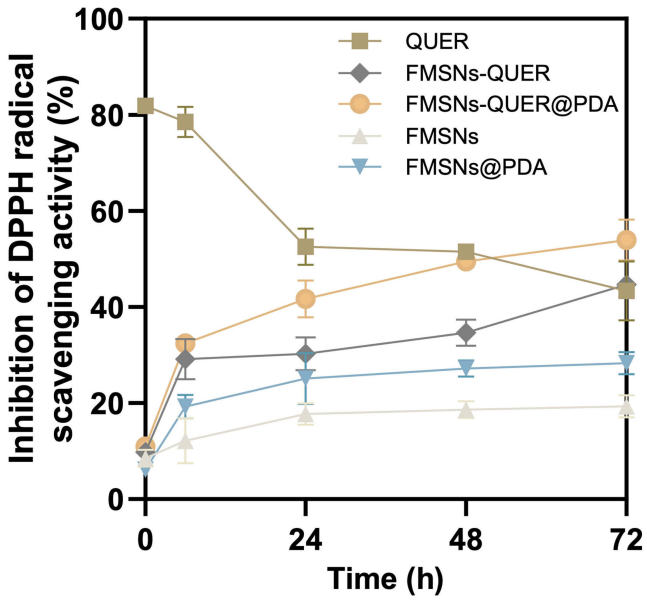

Figure 4 Radical-scavenging activity of QUER, FMSNs, FMSNs@PDA, FMSNs-QUER, and FMSNs-QUER@PDA at 0, 6, 24, 48, and 72 h as detected using a DPPH assay. Each value represents the mean ± standard deviation (n = 3).

Although FMSNs lacking the drug exhibited antioxidant capacity, their magnitudes were modest. In contrast, FMSNs@PDA exhibited a discernibly potent radical-scavenging capacity, suggesting that PDA possesses inherent radical-scavenging capabilities. The antioxidant potential inherent in PDA has also been harnessed in the context of nanoparticles, demonstrating its utility in wound healing applications.[56] Thus, the PDA coating imparts additional antioxidant benefits besides modulating drug release kinetics. This enhancement creates a multifaceted mechanism whereby PDA-coated FMSNs contribute to prolonged drug retention and enhanced antioxidant potential, exhibiting a dual-benefit paradigm.

Upon exposure to the external environment, QUER exhibited an initial increase in antioxidant potential, which was quickly followed by a decrease. Conversely, the antioxidant efficacy of QUER encapsulated in nanoparticles gradually increased over time, maintaining a remarkably high potency for up to 72 h. The gradual release of QUER from the nanoparticles facilitated the steady and consistent delivery of highly stable antioxidants to the surrounding milieu. Notably, FMSNs-QUER@PDA exhibited enhanced radical-scavenging activity compared to unencapsulated QUER at 48 h, whereas FMSNs-QUER demonstrated superior antioxidant performance compared to unencapsulated QUER at 72 h. Although using unencapsulated QUER may be sufficient for short-term applications, our results underscore the efficacy of QUER nanoparticle encapsulation in achieving sustained effects in biological systems. Furthermore, our investigation highlights the potential of PDA coatings for their inherent radical-scavenging properties to synergistically complement the long-term drug release mechanism of nanoparticle-encapsulated drugs. This integrated approach offers a versatile strategy for optimizing therapeutic outcomes by exploiting the inherent properties of QUER and the additional benefits of nanoparticle encapsulation and PDA coating.

The 3T3-L1 cell line was chosen for this study due to its well-established role as a model system for adipogenesis and lipid metabolism research. These cells have been widely used to study the molecular mechanisms of adipocyte differentiation and to evaluate the effects of various compounds on adipogenesis.[57] Therefore, the use of 3T3-L1 cells in our study provides a relevant and reliable model to evaluate the potential of FMSNs-QUER in inhibiting adipogenesis and addressing obesity-related concerns.

MTT assays were performed on days 1, 4, and 7 to evaluate the effects of QUER, FMSNs-QUER, and FMSNs-QUER@PDA on cell proliferation (Figure 5). In the control group, cells proliferated gradually over time. QUER showed an absorbance level similar to the control at all concentrations, indicating that QUER did not affect the proliferation of 3T3-L1 cells prior to differentiation. In contrast, cells in the FMSNs-QUER group showed reduced cell proliferation than those in the control group at all concentrations, although they showed an increasing trend over time. The PDA-coated FMSNs-QUER@PDA group had similar absorbance values to FMSNs-QUER on day 1 but had significantly higher cell proliferation over time. However, the cell proliferation in this group was still lower than that in the control and QUER groups.

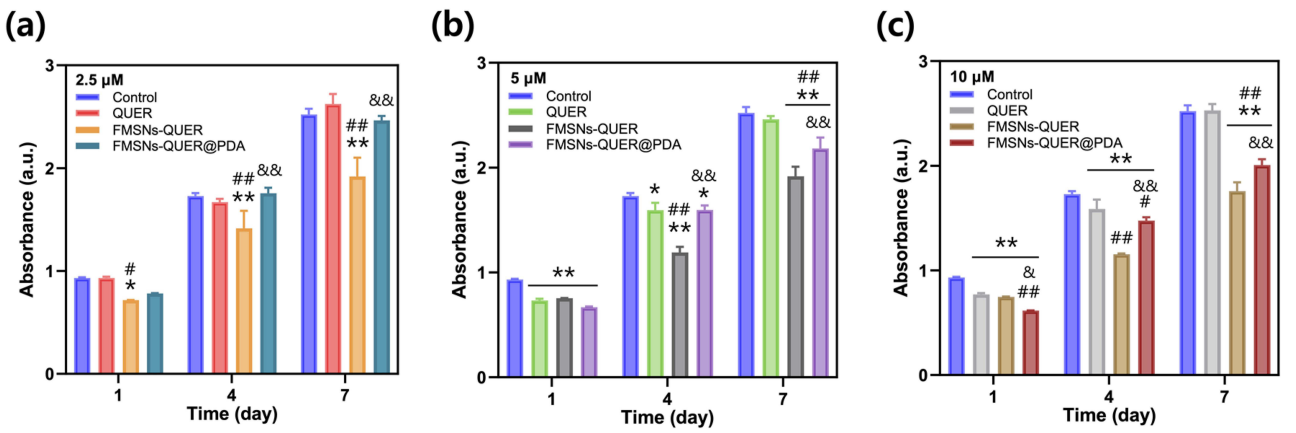

Figure 5 Viability of 3T3-L1 cells after treatment with QUER, FMSNs, FMSNs@PDA, FMSNs-QUER, and FMSNs-QUER@PDA at concentrations of (**a**) 2.5 μM, (**b**) 5 μM, and (**c**) 10 μM on days 1, 4, and 7 as detected using the MTT assay. Each value represents the mean ± standard deviation (n = 3). Significant differences are indicated as 0.01<p<0.05 (*, #, and), p<0.01 (**, ##, andand). The symbols *, #, and and indicate differences from the control, QUER, and FMSNs-QUER groups for each concentration, respectively.

The relatively low proliferation levels common to the FMSN-coated groups may be, in part, due to the physical blockage of oxygen or nutrients on the cell surface by the nanoparticles, which inhibits cell proliferation.[58] When the particles were coated with PDA, there was a slight increase in cell proliferation, despite the potential exacerbation of the physical blockage of oxygen or nutrients by the PDA coating. This increase in cell proliferation may be attributed to the enhanced cell adhesion and intracellular influx properties of PDA, which could promote cell growth and survival.

To elucidate the influence of the PDA coating on cellular uptake, a detailed evaluation of cellular uptake was performed. This study involved the fluorescence tracking of FMSNs over time, confirming intracellular particle uptake via fluorescence imaging (Figure 6). Analyzing the cellular absorption area using ImageJ measurements, the first day showed similar cellular uptake for both FMSNs and FMSNs@PDA. However, one day later, FMSNs@PDA showed increased absorption rates, indicating the ability of PDA to enhance particle uptake over time. This phenomenon was attributed to the properties of PDA, which has a positively charged surface capable of interacting with the negatively charged phosphate groups within the lipid bilayer.[59]

On the second day, the spent medium was replaced, which resulted in the removal of particles not absorbed by the cells; hence, a significant decrease in coverage was observed on day 4. Impressively, even after the medium was changed again on day 4, the coverage remained constant on day 6, indicating the persistence of all particles that had entered the cells. These results confirmed the efficacy of PDA-coated nanoparticles as a viable delivery strategy to circumvent the inherent limitations of QUER, particularly its limited solubility and permeability.

Chou et al showed that the fluorescence of fluorescent organosilica nanoparticles was maintained for more than 2 days after uptake into cells.[60] The study confirmed that the fluorescence was maintained in the cells for 6 days, indicating the stability and persistence of the FMSNs and FMSNs@PDA within the cellular environment. The PDA coating enhances the internalization of the nanoparticles by the cells and improves drug uptake.[61] This increase in intracellular drug uptake could lead to higher intracellular drug concentrations and longer intracellular retention times, which may contribute to the enhanced therapeutic efficacy of FMSNs-QUER@PDA.

In conclusion, this study substantiated the influential role of particle characteristics, particularly the PDA coating, in modulating cellular uptake and intracellular persistence of FMSNs. The PDA coating significantly enhanced the cellular internalization of FMSNs, highlighting the potential of PDA-coated nanoparticles to mitigate potential adverse effects by enhancing particle entry into cells. These findings provide valuable insight into the design and optimization of nanocarrier systems for efficient drug delivery and improved therapeutic outcomes.

We induced the differentiation of 3T3-L1 cells into adipocytes using adipogenic inducers to determine lipid generation. The cellular uptake of QUER was also investigated to determine its potential to inhibit adipocyte differentiation. A differentiation cocktail consisting of insulin, IBMX, and dexamethasone was administered with the compound for eight days to induce adipocyte differentiation in 3T3-L1 cells. Oil Red O staining was performed to compare the extent of adipocyte differentiation. Adipocyte differentiation results in the formation of lipid droplets in which the lipophilic dye Oil Red O, characterized by its red hue,

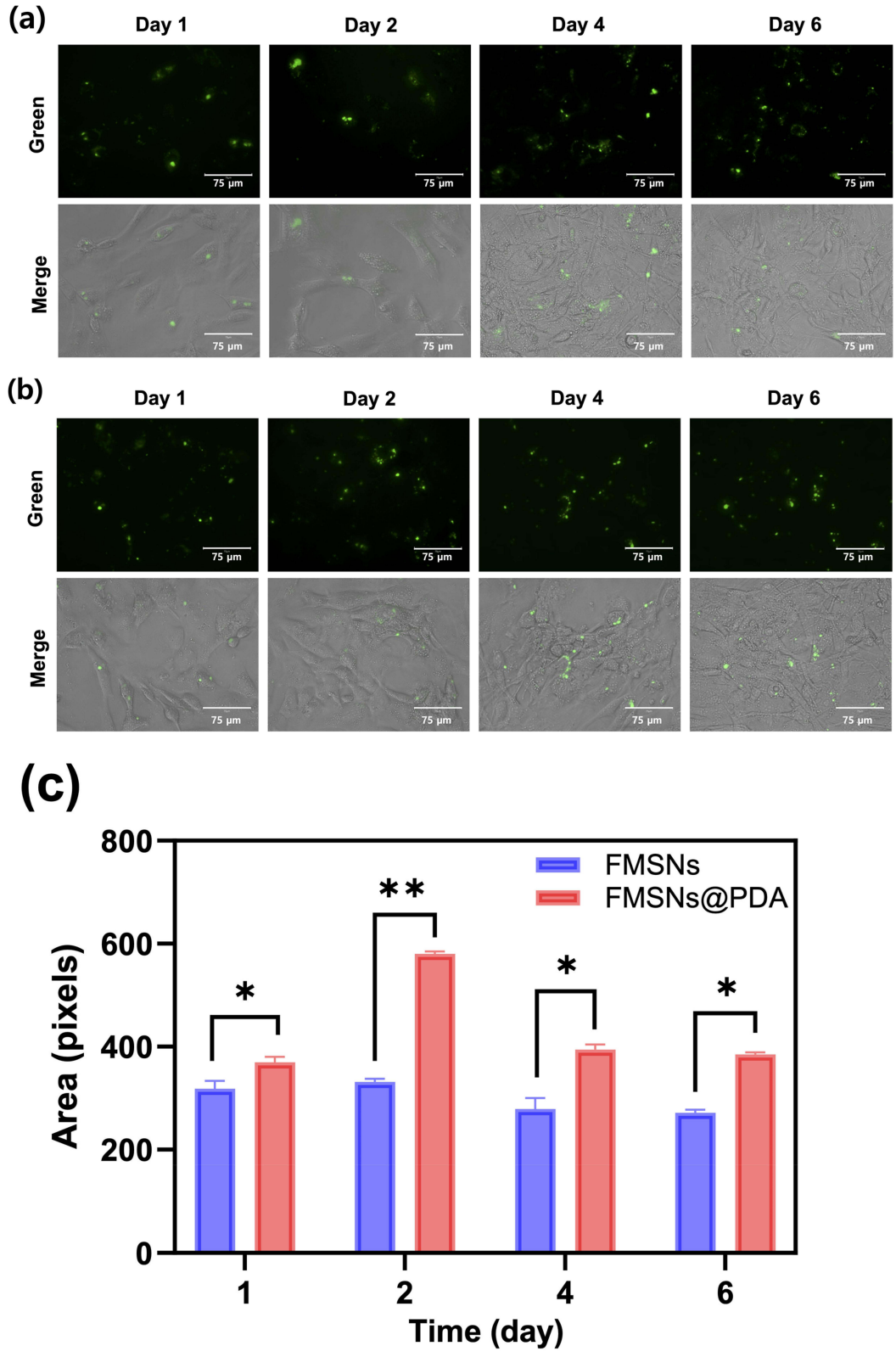

Figure 6 Fluorescence images of (**a**) FMSNs and (**b**) FMSNs@PDA on days 1, 2, 4, and 6. Scale bars = 75 μM. (**c**) Uptake area of FMSNs and FMSNs@PDA. Significant differences are indicated as 0.01<p<0.05 (*), p<0.01 (**). The symbol * indicates a difference from the FMSNs.

dissolves in the lipids, thereby facilitating staining.[62] This technique allows visualization and quantification of lipid accumulation in differentiated adipocytes, which is a hallmark of adipogenesis. Oil Red O staining is a critical method used in this study to evaluate the inhibitory effect of FMSNs-QUER on adipogenesis.

Comparing the area of the Oil Red O-stained regions with that of the non-treated control group, all QUER-treated groups showed a reduction in the stained area and weaker red staining (Figure 7a). This observation indicated a decrease in lipid accumulation due to the inhibitory effect of QUER on adipocyte differentiation. For quantitative analysis, the red intensity of the captured images was measured and compared using ImageJ software (Figure 7b). After normalizing the red intensity analysis value of the control group to 100, QUER concentrations of 2.5, 5, and 10 μM showed relative intensities of 47.5 ± 3.8, 46.1 ± 5.0, and 50.1 ± 3.8, respectively. FMSNs-QUER showed relative intensities of 55.2 ± 5.4,

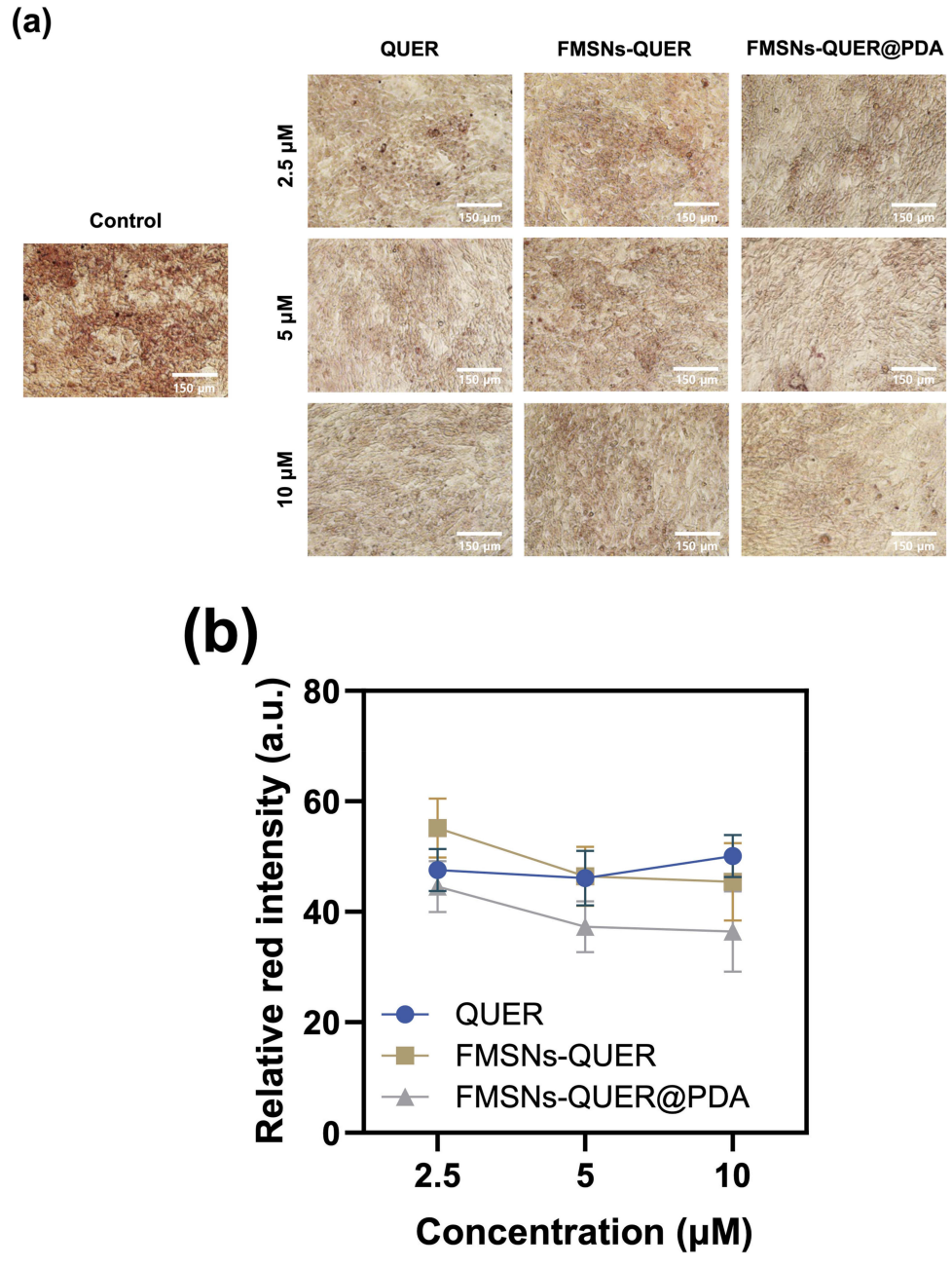

Figure 7 Effects of QUER on the inhibition of 3T3-L1 adipogenesis. (**a**) Optical images of 3T3-L1 adipocytes treated with different concentrations of QUER, FMSNs-QUER, and FMSNs-QUER@PDA. Lipids were stained with Oil Red O on day 8. Scale bar = 150 μm. (**b**) Relative intensities measured using ImageJ software. The red intensity of the control group was set to 100, and the remaining groups were normalized to the intensity of the control group.

46.4 ± 5.3, and 45.4 ± 7.0 for each concentration, respectively, while FMSNs-QUER@PDA showed relative intensities of 44.6 ± 4.6, 37.3 ± 4.6, and 36.5 ± 7.3, respectively.

In all concentration ranges, FMSNs-QUER@PDA demonstrated superior adipogenesis inhibitory efficacy compared to free QUER and FMSNs-QUER. Regardless of the concentration, free QUER showed consistent levels of adipogenesis inhibition. Due to its high lipophilicity and low aqueous solubility, QUER has inherent limitations in terms of low bioavailability. Consequently, this experimental result confirms that increasing the concentration of free QUER does not significantly improve adipogenesis inhibition in 3T3-L1 cells.

Conversely, QUER loaded onto FMSNs showed an increase in adipogenesis inhibition with increasing concentrations. Loading QUER onto particles allows for sustained delivery, resulting in superior efficacy compared to free QUER, especially at higher concentrations. When comparing FMSNs-QUER and FMSNs-QUER@PDA, the enhancement of adipogenesis inhibition by PDA coating was evident. The PDA coating increased particle uptake, allowing higher concentrations of QUER to be maintained inside the cells. Consequently, this leads to improved drug delivery efficiency and enhanced therapeutic effects.

In conclusion, the use of nanoparticles and PDA coating to improve the stability and biocompatibility of QUER is expected to provide enhanced practical efficacy in real-world scenarios. The results provide a holistic perspective on the potential of these nanocarriers to advance drug delivery strategies for the treatment of obesity-related diseases by integrating nanotechnology, bioactive compounds, and therapeutic concepts for innovative precision medicine. The superior adipogenesis inhibition efficacy of FMSNs-QUER@PDA highlight the importance of nanocarrier design and surface modification in optimizing the therapeutic of natural compounds like QUER.

Conclusion

We successfully developed a tailored drug delivery system using FMSNs for efficient delivery of QUER to inhibit adipogenesis. The PDA coating on FMSNs enhanced the antioxidant efficacy and cellular uptake of the nanocarriers, resulting in improved therapeutic effects. This study highlights the advantages of using mesoporous nanocarriers for sustained drug release and targeted delivery, which can be further enhanced by surface modifications such as PDA coating. However, the long-term stability and potential toxicity of the nanocarriers should be investigated in future studies. In addition, in vivo experiments are needed to validate the therapeutic efficacy of QUER-loaded FMSNs in animal models of obesity and related disorders. Despite these limitations, our findings provide valuable insights into the design and development of effective nanomedicine strategies for the treatment of obesity and oxidative stress-related diseases.

Abbreviations

3-aminopropyl-trimethoxysilane, APTMS; 3-isobutyl-1-methylxanthine, IBMX; 3-(4,5-dimethylthiazol-2-yl)-2,5-diphenyltetrazolium bromide, MTT; APTMS-FITC complex, A-F complex; Barrett–Joyner–Halenda, BJH; Bovine calf serum, BCS; Brunauer–Emmett–Teller, BET; Cetyltrimethylammonium bromide, CTAB; Dimethyl sulfoxide, DMSO; Dopamine hydrochloride, DA; Dulbecco's modified Eagle medium, DMEM; Electrophoretic light scattering, ELS; Fetal bovine serum, FBS; Fluorescein isothiocyanate, FITC; Fluorescent mesoporous silica nanoparticles, FMSNs; Fourier-transform infrared, FT-IR; Hydrochloric acid, HCl; Mesoporous silica nanoparticles, MSNs; Phosphate-buffered saline, PBS; Photoluminescence, PL; Polydopamine, PDA; Poly(lactic-co-glycolic acid), PLGA; Quercetin, QUER; Scanning electron microscopy, SEM; Solid lipid nanoparticles, SLNs; Tetraethyl orthosilicate, TEOS; Transmission electron microscopy, TEM; Tris-(hydroxymethyl)aminomethane-HCl buffer, Tris-HCl; X-ray diffraction, XRD; 2.2-diphenyl-1-picrylhydrazyl, DPPH.

Acknowledgments

This work was supported by the National Research Foundation of Korea (NRF) (NRF-2021R1A6A1A03038996) and the Basic Science Research Capacity Enhancement Project through a Korea Basic Science Institute (National Research Facilities and Equipment Center) (2019R1A6C1010016) grant funded by the Ministry of Science and ICT (MSIT). This study was partially supported by the Gachon University Research Fund (GCU-202301050001).

Disclosure

The authors report no conflicts of interest in this work.

References

1. Kassie AM, Abate BB, Kassaw MW. Prevalence of overweight/obesity among the adult population in Ethiopia: a systematic review and meta-analysis. *BMJ Open*. 2020;10(8):e039200. doi:10.1136/bmjopen-2020-039200
2. Atella V, Piano Mortari A, Kopinska J, et al. Trends in age-related disease burden and healthcare utilization. *Aging Cell*. 2019;18(1):e12861. doi: doi:10.1111/acel.12861
3. Müller TD, Blüher M, Tschöp MH, DiMarchi RD. Anti-obesity drug discovery: advances and challenges. *Nat Rev Drug Discov*. 2022;21 (3):201–223. doi:10.1038/s41573-021-00337-8
4. Abdi Beshir S, Ahmed Elnour A, Soorya A, et al. A narrative review of approved and emerging anti-obesity medications. *Saudi Pharm J*. 2023;31 (10):101757. doi:10.1016/j.jsps.2023.101757
5. Garg SK, Maurer H, Reed K, Selagamsetty R. Diabetes and cancer: two diseases with obesity as a common risk factor. *Diabetes Obes Metab*. 2014;16(2):97–110. doi:10.1111/dom.12124
6. Jakab J, Miškić B, Mikšić Š, et al. Adipogenesis as a potential anti-obesity target: a review of pharmacological treatment and natural products. *Diabetes Metab Syndr Obes*. 2021;14:67–83. doi:10.2147/dmso.S281186
7. Brandfon S, Eylon A, Khanna D, Parmar MS. Advances in anti-obesity pharmacotherapy: current treatments, emerging therapies, and challenges. *Cureus*. 2023;15(10):e46623. doi:10.7759/cureus.46623
8. Hidalgo M, Sánchez-Moreno C, de Pascual-Teresa S. Flavonoid–flavonoid interaction and its effect on their antioxidant activity. *Food Chem*. 2010;121(3):691–696. doi:doi:10.1016/j.foodchem.2009.12.097
9. Wang W, Sun C, Mao L, et al. The biological activities, chemical stability, metabolism and delivery systems of quercetin: a review. *Trends Food Sci Technol*. 2016;56:21–38. doi:doi:10.1016/j.tifs.2016.07.004
10. Harmon AW, Harp JB. Differential effects of flavonoids on 3T3-L1 adipogenesis and lipolysis. *Am J Physiol Cell Physiol*. 2001;280(4):C807–13. doi:10.1152/ajpcell.2001.280.4.C807
11. Rajesh RU, Dhanaraj S. A critical review on quercetin bioflavonoid and its derivatives: scope, synthesis, and biological applications with future prospects. *Arabian J Chem*. 2023;16(8):104881. doi:doi:10.1016/j.arabjc.2023.104881
12. Xu D, Hu M-J, Wang Y-Q, Cui Y-L. Antioxidant activities of quercetin and its complexes for medicinal application. *Molecules*. 2019;24(6):1123. doi:10.3390/molecules24061123
13. Salehi B, Machin L, Monzote L, et al. Therapeutic potential of quercetin: new insights and perspectives for human health. *ACS Omega*. 2020;5 (20):11849–11872. doi:10.1021/acsomega.0c01818
14. Kandemir K, Tomas M, McClements DJ, Capanoglu E. Recent advances on the improvement of quercetin bioavailability. *Trends Food Sci Technol*. 2022;119:192–200. doi:10.1016/j.tifs.2021.11.032
15. Walle T. Absorption and metabolism of flavonoids. *Free Radic Biol Med*. 2004;36(7):829–837. doi:10.1016/j.freeradbiomed.2004.01.002
16. Wang S, Su R, Nie S, et al. Application of nanotechnology in improving bioavailability and bioactivity of diet-derived phytochemicals. *J Nutr Biochem*. 2014;25(4):363–376. doi:10.1016/j.jnutbio.2013.10.002
17. Giannouli M, Karagkiozaki V, Pappa F, Moutsios I, Gravalidis C, Logothetidis S. Fabrication of quercetin-loaded PLGA nanoparticles via electrohydrodynamic atomization for cardiovascular disease. *Mater Today Proc*. 2018;5(8, Part 2):15998–16005. doi:10.1016/j.matpr.2018.05.044
18. Pi J, Li B, Tu L, et al. Investigation of quercetin-induced HepG2 cell apoptosis-associated cellular biophysical alterations by atomic force microscopy. *Scanning*. 2016;38(2):100–112. doi:10.1002/sca.21245
19. Kıyga E, Şengelen A, Adıgüzel Z, Önay Uçar E. Investigation of the role of quercetin as a heat shock protein inhibitor on apoptosis in human breast cancer cells. *Mol Bio Rep*. 2020;47(7):4957–4967. doi:10.1007/s11033-020-05641-x
20. Zhou Y, Chen D, Xue G, et al. Improved therapeutic efficacy of quercetin-loaded polymeric nanoparticles on triple-negative breast cancer by inhibiting uPA. 10.1039/D0RA04231E. *RSC Adv*. 2020;10(57):34517–34526. doi:10.1039/D0RA04231E
21. Talarico L, Consumi M, Leone G, Tamasi G, Magnani A. Solid lipid nanoparticles produced via a coacervation method as promising carriers for controlled release of quercetin. *Molecules*. 2021;26(9):2694. doi:10.3390/molecules26092694
22. Weerapol Y, Manmuan S, Chaothanaphat N, et al. New approach for preparing solid lipid nanoparticles with volatile oil-loaded quercetin using the phase-inversion temperature method. *Pharmaceutics*. 2022;14(10):1984. doi:10.3390/pharmaceutics14101984
23. Chaudhari VS, Gawali B, Saha P, Naidu VGM, Murty US, Banerjee S. Quercetin and piperine enriched nanostructured lipid carriers (NLCs) to improve apoptosis in oral squamous cellular carcinoma (FaDu cells) with improved biodistribution profile. *Eur J Pharmacol*. 2021;909:174400. doi:10.1016/j.ejphar.2021.174400
24. Sun M, Nie S, Pan X, Zhang R, Fan Z, Wang S. Quercetin-nanostructured lipid carriers: characteristics and anti-breast cancer activities in vitro. *Colloids Surf. B*. 2014;113:15–24. doi:10.1016/j.colsurfb.2013.08.032
25. Niemelä E, Desai D, Nkizinkiko Y, Eriksson JE, Rosenholm JM. Sugar-decorated mesoporous silica nanoparticles as delivery vehicles for the poorly soluble drug celastrol enables targeted induction of apoptosis in cancer cells. *Eur J Pharm Biopharm*. 2015;96:11–21. doi:10.1016/j.ejpb.2015.07.009
26. Wang Y, Zhao Q, Han N, et al. Mesoporous silica nanoparticles in drug delivery and biomedical applications. *Nanomed Nanotechnol Biol Med*. 2015;11(2):313–327. doi:10.1016/j.nano.2014.09.014
27. Li H, Jia Y, Peng H, Li J. Recent developments in dopamine-based materials for cancer diagnosis and therapy. *Adv. Colloid Interface Sci.* 2018;252:1–20. doi:10.1016/j.cis.2018.01.001
28. Li X, Garamus VM, Li N, et al. Preparation and characterization of a pH-responsive mesoporous silica nanoparticle dual-modified with biopolymers. *Colloids Surf. A*. 2018;548:61–69. doi:10.1016/j.colsurfa.2018.03.047
29. Gullotti E, Park J, Yeo Y. Polydopamine-based surface modification for the development of peritumorally activatable nanoparticles. *Pharm Res*. 2013;30(8):1956–1967. doi:10.1007/s11095-013-1039-y

30. Ryu JH, Messersmith PB, Lee H. Polydopamine surface chemistry: a decade of discovery. *ACS Appl Mater Interfaces*. 2018;10(9):7523–7540. doi:10.1021/acsami.7b19865
31. Carucci C, Sechi G, Piludu M, Monduzzi M, Salis A. A drug delivery system based on poly-L-lysine grafted mesoporous silica nanoparticles for quercetin release. *Colloids Surf. A*. 2022;648:129343. doi:10.1016/j.colsurfa.2022.129343
32. Moon YJ, Wang L, DiCenzo R, Morris ME. Quercetin pharmacokinetics in humans. *Biopharm Drug Dispos*. 2008;29(4):205–217. doi:10.1002/bdd.605
33. Wang C, Zhao T, Li Y, Huang G, White MA, Gao J. Investigation of endosome and lysosome biology by ultra pH-sensitive nanoprobes. *Adv Drug Deliv Rev*. 2017;113:87–96. doi:10.1016/j.addr.2016.08.014
34. Son MJ, Kim T, Lee S-W. Facile synthesis of fluorescent mesoporous nanocarriers with pH-sensitive controlled release of naturally derived dieckol. *Colloids Surf. A*. 2023;657:130535. doi:10.1016/j.colsurfa.2022.130535
35. Lai S-M, Tsai T-Y, Hsu C-Y, Tsai J-L, Liao M-Y, Lai P-S. Bifunctional silica-coated superparamagnetic FePt nanoparticles for fluorescence/MR dual imaging. *J Nanomater*. 2012;2012:5. doi:10.1155/2012/631584
36. Liu Q, Yu B, Ye W, Zhou F. Highly selective uptake and release of charged molecules by ph-responsive polydopamine microcapsules. *Macromol biosci*. 2011;11(9):1227–1234. doi:10.1002/mabi.201100061
37. Duan M, Tang Q, Wang M, et al. Preparation of poly-dopamine-silk fibroin sponge and its dye molecular adsorption. *Wat Sci Technol*. 2020;82(11):2353–2365. doi:10.2166/wst.2020.502
38. Tadjarodi A, Zabihi F, Afshar S. Experimental investigation of thermo-physical properties of platelet mesoporous SBA-15 silica particles dispersed in ethylene glycol and water mixture. *Ceram. Int*. 2013;39(7):7649–7655. doi:10.1016/j.ceramint.2013.02.103
39. Ursachi I, Vasile A, Ianculescu A, Vasile E, Stancu A. Ultrasonic-assisted synthesis and magnetic studies of iron oxide/MCM-41 nanocomposite. *Mater Chem Phys*. 2011;130(3):1251–1259. doi:10.1016/j.matchemphys.2011.09.004
40. Tran VA, Lee S-W. A prominent anchoring effect on the kinetic control of drug release from mesoporous silica nanoparticles (MSNs). *J Colloid Interface Sci*. 2018;510:345–356. doi:10.1016/j.jcis.2017.09.072
41. Y-L W, Han Z-F, Yan X, Lang W-Z, Guo Y-J. Effective synthesis of vanadium-doped mesoporous silica nanospheres by sol-gel method for propane dehydrogenation reaction. *Microporous Mesoporous Mater*. 2022;330:111616. doi:10.1016/j.micromeso.2021.111616
42. Rahoui N, Jiang B, Hegazy M, et al. Gold modified polydopamine coated mesoporous silica nano-structures for synergetic chemo-photothermal effect. *Colloids Surf. B*. 2018;171:176–185. doi:10.1016/j.colsurfb.2018.07.015
43. Muhammad F, Guo M, Qi W, et al. pH-triggered controlled drug release from mesoporous silica nanoparticles via intracelluar dissolution of ZnO Nanolids. *J Am Chem Soc*. 2011;133(23):8778–8781. doi:10.1021/ja200328s
44. Fusina A, Degot P, Touraud D, Kunz W, Nardello-Rataj V. Enhancement of water solubilization of quercetin by meglumine and application of the solubilization concept to a similar system. *J Mol Liq*. 2022;368:120756. doi:10.1016/j.molliq.2022.120756
45. Xu Z, Hu L, Ming J, et al. Self-gated porous organic polymer as drug delivery system for pH stimuli-responsive controlled Quercetin release. *Microporous Mesoporous Mater*. 2020;303:110259. doi:10.1016/j.micromeso.2020.110259
46. Foti MC, Daquino C, DiLabio GA, Ingold KU. Kinetics of the oxidation of quercetin by 2,2-diphenyl-1-picrylhydrazyl (dpph•). *Organic Letters*. 2011;13(18):4826–4829. doi:10.1021/ol2019086
47. Sunoqrot S, Al-Shalabi E, Messersmith PB. Facile synthesis and surface modification of bioinspired nanoparticles from quercetin for drug delivery. 10.1039/C8BM00587G. *Biomater. Sci.* 2018;6(10):2656–2666. doi:10.1039/C8BM00587G
48. Klitou P, Rosbottom I, Simone E. Synthonic modeling of quercetin and its hydrates: explaining crystallization behavior in terms of molecular conformation and crystal packing. *Cryst. Growth Des.* 2019;19(8):4774–4783. doi:10.1021/acs.cgd.9b00650
49. Saputra OA, Lestari WA, Kurniansyah V, et al. Organically surface engineered mesoporous silica nanoparticles control the release of quercetin by pH stimuli. *Sci Rep*. 2022;12(1):20661. doi:10.1038/s41598-022-25095-4
50. Zheng Q, Lin T, Wu H, et al. Mussel-inspired polydopamine coated mesoporous silica nanoparticles as pH-sensitive nanocarriers for controlled release. *Int J Pharm*. 2014;463(1):22–26. doi:10.1016/j.ijpharm.2013.12.045
51. Chang D, Gao Y, Wang L, et al. Polydopamine-based surface modification of mesoporous silica nanoparticles as pH-sensitive drug delivery vehicles for cancer therapy. *J Colloid Interface Sci*. 2016;463:279–287. doi:10.1016/j.jcis.2015.11.001
52. Lim E-B, Vy TA, Lee S-W. Comparative release kinetics of small drugs (ibuprofen and Acetaminophen) from multifunctional mesoporous silica nanoparticles. 10.1039/C9TB02494H. *J Mat Chem B*. 2020;8(10):2096–2106. doi:10.1039/C9TB02494H
53. Min Jeong K, Ji Hyun K, Sanghyun L, Eun Ju C, Hyung Young K. Determination of radical scavenging activity of aster yomena (Kitam.) *honda. determination of radical scavenging activity of aster yom*ena (Kitam.) honda. *J Korea Aca-Indus Soc*. 2018;19(9):402–407.
54. Martemucci G, Costagliola C, Mariano M, D'andrea L, Napolitano P, D'Alessandro AG. Free radical properties, source and targets, antioxidant consumption and health. *Oxygen*. 2022;2(2):48–78. doi:10.3390/oxygen2020006
55. Choi SI, Lee JS, Lee S, et al. Radical scavenging-linked anti-adipogenic activity of alnus firma extracts. *Int J Mol Med*. 2018;41(1):119–128. doi:10.3892/ijmm.2017.3221
56. Hu J, Yang L, Yang P, Jiang S, Liu X, Li Y. Polydopamine free radical scavengers. 10.1039/D0BM01070G. *Biomater. Sci.* 2020;8(18):4940–4950. doi:10.1039/D0BM01070G
57. Ruiz-Ojeda FJ, Rupérez AI, Gomez-Llorente C, Gil A, Aguilera CM. Cell models and their application for studying adipogenic differentiation in relation to obesity: a review. *Int J Mol Sci*. 2016;17(7):1040. doi:10.3390/ijms17071040
58. Barua S, Mitragotri S. Challenges associated with penetration of nanoparticles across cell and tissue barriers: a review of current status and future prospects. *Nano Today* 2014. 9(2):223–243. doi:10.1016/j.nantod.2014.04.008
59. Hu S, Pei X, Duan L, et al. A mussel-inspired film for adhesion to wet buccal tissue and efficient buccal drug delivery. *Nat Commun*. 2021;12(1):1689. doi:10.1038/s41467-021-21989-5
60. Chou H-C, Chiu S-J, T-M H. Quantitative analysis of macrophage uptake and retention of fluorescent organosilica nanoparticles. *bioRxiv*. 2023;2023.06.12.544701. doi:10.1101/2023.06.12.544701
61. Busa P, Koutavarapu R, Kuthati Y. Polydopamine-coated copper-substituted mesoporous silica nanoparticles for dual cancer therapy. *Coatings*. 2022;12(1):60. doi:10.3390/coatings12010060
62. Park MJ, Song JH, Shon MS, et al. Anti-adipogenic effects of ethanol extracts prepared from selected medicinal herbs in 3t3-l1 cells. *Prev Nutr Food Sci*. 2016;21(3):227–235. doi:10.3746/pnf.2016.21.3.227